Title: **Cerebral collateral flow defines topography and evolution of molecular penumbra in experimental ischemic stroke**

Simone Beretta [a,f*], Elisa Cuccione [a,b*], Alessandro Versace [a], Davide Carone [a], Matteo Riva [a], Giada Padovano [a], Valentina Dell'Era [a], Ruiyao Cai [a], Laura Monza [a], Luca Presotto [c,d], David Rousseau [e], Fabien Chauveau [e], Giovanni Paternò [a], Giovanni B. Pappadà [a], Carlo Giussani [a], Erik P. Sganzerla [a] , Carlo Ferrarese [a,f]

[a] Laboratory of Experimental Stroke Research, Department of Surgery and Translational Medicine, University of Milano Bicocca, Monza, Italy

[b] PhD Programme in Neuroscience, University of Milano Bicocca, Monza, Italy

[c] Department of Nuclear Medicine, San Raffaele Scientific Institute, Milan, Italy

[d] Institute of Bioimaging and Molecular Physiology, National Research Council, Milan, Italy

[e] Université de Lyon, CREATIS; CNRS UMR5220; Inserm U1044; INSA-Lyon; Université Lyon 1, France

[f] Milan Center for Neuroscience (NeuroMi), Milano, Italy

[*]These authors equally contributed to this work

Corresponding author:

Dr. Simone Beretta, MD, PhD

Laboratory of Experimental Stroke Research

Department of Surgery and Translational Medicine

University of Milano Bicocca

Via Cadore 48, 20900 Monza (MI) – Italy

Phone: +390264488128 Fax: +390264488108

e-mail: simone.beretta@unimib.it

Abstract

Intracranial collaterals are dynamically recruited after arterial occlusion and are emerging as a strong determinant of tissue outcome in both human and experimental ischemic stroke. The relationship between collateral flow and ischemic penumbra remains largely unexplored in pre-clinical studies. The aim of the present study was to investigate the pattern of collateral flow with regard to penumbral tissue after transient middle cerebral artery (MCA) occlusion in rats. MCA was transiently occluded (90 minutes) by intraluminal filament in adult male Wistar rats (n=25). Intracranial collateral flow was studied in term of perfusion deficit and biosignal fluctuation analysis using multi-site laser Doppler monitoring. Molecular penumbra was defined by topographical mapping and quantitative signal analysis of Heat Shock Protein 70 kDa (HSP70) immunohistochemistry. Functional deficit and infarct volume were assessed 24 hours after ischemia induction. The results show that functional performance of intracranial collaterals during MCA occlusion inversely correlated with HSP70 immunoreactive areas in both cortex and striatum, as well as with infarct size and functional deficit. Intracranial collateral flow was associated with reduced areas of both molecular penumbra and ischemic core and increased areas of intact tissue in rats subjected to MCA occlusion followed by reperfusion. Our findings prompt the development of collateral therapeutics to provide tissue-saving strategies in the hyper-acute phase of ischemic stroke prior to recanalization therapy.

Keywords: stroke; penumbra; cerebral collaterals; hemodynamic changes; neuroprotection

Introduction

Intracranial collateral circulation represents a multiple-level subsidiary vascular network which is dynamically recruited after occlusion of cerebral arteries to provide a source of residual blood flow (Liebeskind et al., 2003).

In both humans and rodents, a significant supply of collateral flow after middle cerebral artery (MCA) occlusion is provided by the circle of Willis through the anterior cerebral artery (ACA) and the leptomeningeal anastomoses between the cortical branches of ACA and MCA. However, a significant degree of inter-individual variability exists in the functional performance of intracranial collaterals under ischemic conditions in humans (Qureshi et al., 2008; Liu et al., 2011) and rodents (Armitage et al., 2010; Riva et al., 2012).

Cerebral collateral flow is emerging as a powerful determinant of functional and tissue outcome in unselected ischemic stroke patients (Maas et al., 2009; Menon et al., 2011) and in stroke patients treated with intravenous rtPA (Brunner et al., 2012; Miteff et al., 2009) or endovascular recanalization (Bang et al., 2011; Bang et al., 2008).

For these reasons, an in-depth understanding of the physiology, adaptive response and modulation of intracranial collateral circulation is of foremost importance for acute stroke pathophysiology and therapy.

Ischemic penumbra was originally defined as “tissue at risk”, which has been made functionally silent and metabolically metastable by ischemic injury but still has the potential for full recovery if reperfusion is timely achieved (Branston et al., 1974; Hossmann et al., 1994; Baron, 1999). The concept of ischemic penumbra is gradually evolving, after pre-clinical and clinical studies showed an heterogeneous and variable pattern of perfusion deficit, molecular response, topographical distribution and evolution of the penumbra in relation to the ischemic core (Del Zoppo et al., 2011; Manning et al., 2014).

HSP70 is the major inducible heat shock protein (Sharp et al., 2000), whose expression after focal cerebral ischemia reflects an endogenous cell response to injury. The neuronal expression of HSP70

is considered as a molecularly defined penumbra, where injured neurons have activated endogenous pathways for protein renaturation and protection against further ischemia.

In the present study, we investigated the relationship between intracranial collateral flow during transient MCA occlusion and the development of molecular penumbra and ischemic infarct after 24 hours. The hemodynamic monitoring of central and peripheral MCA territory was analyzed in term of perfusion deficit and biosignal fluctuation. Hemodynamic data were correlated with the corresponding areas of molecular penumbra, infarct volume and functional deficit.

Material and Methods

Study design

The experimental protocol was approved by the Committee on Animal Care of the University of Milano Bicocca, in accordance with the national guidelines on the use of laboratory animals (D.L. 116/1992) and the European Union Directive for animal experiments (2010/63/EU), under project licence from the Italian Ministry of Health.

A group of consecutive animals undergoing successful MCA occlusion (see below) were used to explore the effect of cerebral collateral flow on molecular penumbra. Cerebral collateral flow (defined by perfusion deficit in the MCA-ACA borderzone territory) was considered as a continuous independent variable. Primary outcome was defined as the quantification of molecular penumbra (HSP70 positive areas). Secondary outcomes were infarct volume and neurobehaviour. Outcome assessment was blinded to hemodynamic data on cerebral collateral flow.

Animals and surgery.

Animals were housed in single cages, exposed to 12/12 hours light/dark cycle, at controlled room temperature, with free access to food and water, in a specific pathogen free (SPF) facility.

Adult male Wistar rats (280±5% g; n = 28) were anesthetized with 3% isoflurane in O_2 /N_2O (1:3), and maintained with 1.5% isoflurane. Occlusion of the origin of the right MCA was induced transiently for 90 minutes with a reperfusion period of 24 hours. Briefly, a silicone-coated filament (diameter 0.39±0.02 mm, Doccol Corporation, Redlands, CA, USA), was introduced in the right external carotid artery and pushed through the right internal carotid artery to occlude the origin of the right MCA. Common carotid artery was transiently occluded immediately before the insertion of the filament and subsequently re-opened during ischemia period and reperfusion. Pterygopalatin artery was transiently occluded for both the surgical insertion of the filament and ischemia, then re-opened during reperfusion.

During surgery, the core temperature of 37°C was controlled by a rectal thermometer connected to a feedback-controlled heating pad. In a subset of animals (n=12) cardio-respiratory parameters (arterial pressure, heart rate, respiratory rate) were continuously monitored using Samba Preclin 420 transducer (Samba Sensors, Harvard Apparatus, UK) inserted in the right femoral artery before ischemia induction.

After reperfusion, rats were allowed to recover and had free access to food and water. After 24 hours from the onset of ischemia, animals were assessed for neurobehavioral score (see below), then euthanized using CO2 inhalation and the brains were collected for fixation.

Three rats were excluded from the experimental series for early death occurred before successful MCA occlusion (one rat died for anesthesiological complications, two rat died for subarachnoid haemorrhage). All successfully occluded rats (n=25) survived the 24 hours reperfusion time and were used for analysis.

Laser doppler multi-site perfusion monitoring.

The induction of focal cerebral ischemia was assessed using laser doppler (LD) perfusion monitoring (dual channel moorVMS-LDF^{TM}, Moor, Axminster, UK) using two blunt needle probes (VP12). Probes were positioned in a custom made silicon holder attached with surgical glue over

the intact skull and further secured in place using sutures to surrounding soft tissues (Beretta et al., 2013). A first probe (Probe 1) was attached to the skull 1 mm posterior to the Bregma and 5 mm lateral to the midline (lateral probe, corresponding to the central MCA territory). A second probe (Probe 2) was attached to the skull 2 mm anterior to the Bregma and 2 mm lateral to the midline (medial probe, corresponding to the borderzone territory between ACA and MCA territory). Cerebral perfusion monitoring was performed continuously during the entire period of anesthesia (approximately 140 minutes), including reperfusion. The mean duration of cerebral perfusion monitoring after reperfusion was 7.8 (4-15) minutes.

Three hemodynamic parameters were considered for signal analysis of each probe: i) drop in cerebral perfusion (expressed as % of baseline) during MCA occlusion following successful filament insertion. ii) biosignal fluctuation analysis during the pre-ischemic period and during MCA occlusion (see below). iii) cerebral reperfusion (expressed as % of baseline), from the removal of the filament until the end of anesthesia.

Hemodynamic assessment was blinded to outcome data (neurobehaviour, infarct volume, HSP70 staining).

Biosignal fluctuation analysis of cerebral perfusion.

Fluctuation analysis of blood microcirculation from LD signals or alternative laser speckle imaging signals has been undertaken with various measures (see Humeau-Heurtier et al., 2013 for a recent review). In this study, auto-correlation *R(k)* analysis was based on linear second order statistics (Humeau et al., 2008), see Supplementary Methods for details.

The auto-correlation *R(k)* measures the selfmemory of the fluctuations around the average value and constitutes an analysis different from the record of the drop of average value between the two probes. As shown in Fig. 2, the two autocorrelation functions estimated for the two probes display a decrease but with a distinct characteristic time decay. To quantify this observation, we compute the time in second that autocorrelation R(k) takes to drop from1 to 0.9 for each probe.

Neurobehavioral assessment.

Rats were assessed 24 hours after transient MCA occlusion with a functional neuroscore for neurological outcome on a scale from 3 (most severe) to 18 (no deficit) (Garcia et al., 1995). Behavioral assessment was blinded to hemodynamic data and consisted of scoring the spontaneous movement, sensory function and motor function.

Histology and infarct volume determination.

Brains were fixed in ice-cold 10% neutral buffer formalin and coronal sections (50 μm) were stained using Cresyl Violet 0.1% (Bioptica, Milano, Italy). Infarct areas were measured in 19 consecutive sections with 250 μm interval (bregma +2.5 mm to -3.0 mm).

Infarct volume was calculated using ImageJ image processing software (National Institute of Health, Bethesda, MD, USA), corrected for inter-hemispheric asymmetries due to cerebral edema, and expressed in mm^3. Infarct volume calculation was blinded to hemodynamic data.

Heat shock protein 70 (HSP70) immunohistochemistry and topography.

Brains were fixed in ice-cold 10% neutral buffer formalin for at least 24 hours. Serial coronal sections (50 μm thick) were obtained using a vibratome throughout its rostro-caudal extension. For each brain, slices anatomically identified as Bregma +1, -1 and -3 were immunoreacted for HSP70. Free-floating coronal sections were pre-incubated for 10 min in 3% H_2O_2 and 30 min in blocking solution (10% normal goat serum) and 0.2% Triton X-100. Sections were then incubated overnight at 4 °C with anti-HSP70 primary antibody (1:1000, mouse anti-HSP70, Enzo LifeScience, Farmingdale, New York, USA) and at room temperature for 75 min with monoclonal Horseradish Peroxidase-conjugated goat anti-mouse IgG (1:200, Millipore, Bellerica, MA, USA). Sections were finally incubated with 3,30-diaminobenzidine tetra hydrochloride (DAB) as chromogen. Negative controls, to verify the specificity of the antibodies, were obtained by omitting primary antibody.

Macroscopic section images were obtained using a digital camera (Nikon Coolpix P5000) adapted to optical microscope. Higher magnification images were obtained using Nikon Eclipse E200 optical microscope and Leica Qwin V3.2.0 software.

HSP70 topography was obtained by manual identification of stained cell clusters in the cortex, whose areas were superimposed to corresponding brain atlas images at Bregma +1, -1 and -3 (Paxinos and Watson, 2007). Each cell cluster is represented by a single pink-coloured area of variable size. A darker pink colour is the result of variable overlapping degree with adjacent areas from different animals. This method of HSP70 qualitative topography was not applied in the striatum, where HSP70-positive cells were mostly present as single cells instead of cell clusters, because of its different cytoarchitecture compared to the cortex.

TUNEL staining, NeuN and HSP70 triple co-immunofluorescence.

Triple labeling was obtained by performing TUNEL assay followed by NeuN and HSP70 immunofluorescence on the same brain sections. TUNEL kit was used following manufacturer instructions (DeadEnd™ Fluorometric TUNEL System, Promega, Madison, WI, USA), except that the tissue permeabilization step was performed using 0.2% Triton X-100 instead of Protease K. After stopping TUNEL reaction, a further step of incubation with 0.1 M glycine in PBS for 15 min was performed. Sections were then incubated with PBS 10% NGS blocking solution at RT for 30 min and overnight at 4 °C with anti-NeuN primary antibody (1:100, mouse anti-NeuN, Merck Millipore (Chemicon), © Merck KGaA, Darmstadt, Germany) and anti-HSP70 primary antibody (1:500, mouse anti-HSP70, Enzo LifeScience, Farmingdale, New York, USA) diluted in PBS 1% NGS. Afterwards sections were incubated at room temperature for 75 min with appropriate fluorochrome-conjugated secondary antibody diluted in PBS 1%NGS (1:200, Alexa Fluor 647 goat anti-mouse, Invitrogen, Oregon, USA and 1:200, Alexa Flour 546 goat anti-rabbit, Invitrogen, Oregon, USA). Sections were then rinsed 3 times for 5 min with PBS 0.1% Triton X-100 and

5mg/mL BSA and finally mounted with polyvinyl alcohol with anti-fading (Polyvinyl Alcohol mounting medium with DABCO® Antifading pH 8,7, Sigma-Aldrich, St. Louis, MO, USA).

Negative controls were obtained by omitting primary antibody for HSP70/NeuN signal or TdT enzyme for TUNEL signal. Microscopy analysis was performed with laser confocal microscopy (Radiance 2100; Biorad Laboratories, Hercules, CA, USA). Noise reduction was achieved by Kalman filtering during acquisition.

HSP70 quantitative immunohistochemistry

A quantitative analysis of the mathematical energy of HSP70 signal was performed as previously described for quantitative immunohistochemistry (Matkowskyj et al., 2000). An in-house program was developed using Matlab software to obtain automated signal energy difference between corresponding regions of interests (ROIs) in the control and ischemic hemisphere. Briefly, HSP70 stained sections anatomically identified as Bregma +1, -1 and -3 were considered. On each section, four regions of interests (ROIs) were identified corresponding to the entire cortical or striatal regions of each hemisphere. We assume that all information contained in the selected ROIs is of importance. In other words, the amount of antibody-generated chromogen is represented by all the information contained in the image file. After acquisition with a digital camera, the file for the experimental image is opened in the Matlab dedicated program. The ROIs are defined using a tool that allows an area of any pixel dimension to be determined by the operator. The same areas were considered for the cortex, as well as the striatum, in each hemisphere (control and ischemic). The "norm" function was used to to compute a unique value of the Energy from a three-colour image, which represents the mathematical energy of the image file. The energy per pixel is estimated by normalizing the measured energy over the whole ROI to the number of pixels included. Finally, the normalized energy of the ischemic ROIs (cortex or striatum) is subtracted to the corresponding control ROIs (cortex or striatum respectively) and expressed as an absolute value.

Gelatin ink perfusion.

In a further set of experiments, rats (n=4) underwent a trans-cardiac perfusion 60 minutes after the induction of cerebral ischemia, without reperfusion (the intraluminal filament was left in place). Normal saline (200 ml) at 37°C was infused first followed by 20 mL of gelatine-ink solution at 37°C (gelatin 3% solution in 0.9% NaCl mixed 1:1 with black ink NSE-40BL, Nihon Kohden, Tokyo, Japan). The brains were then removed and fixed in 10% neutral buffer formalin. To enhance the contrast between ischemic and non-ischemic tissue, brains were imaged using colour inversion.

Sample size determination and statistical analysis

We planned this study with 25 animals in which we regressed their values of collateral flow perfusion against HSP70 immunohistochemistry intensity signal. Our previous data indicated that the standard deviation of HSP70 signal was 0.5. Aiming for a slope of the line obtained by regressing collateral flow perfusion against HSP70 signal above 0.4 to be considered of interest and a regression errors below 0.3, we were able to reject the null hypothesis that this slope equals zero with probability (power) 0.89. The Type I error probability associated with this test of this null hypothesis was 0.05.

Values were expressed as mean ± standard deviation (SD). For two-group analysis unpaired Student's *t* test was used. Correlation and linear regression analyses were computed with Pearson's *r* test. A value of $p < 0.05$ was considered significant.

Results

Multi-site cerebral perfusion monitoring during MCA occlusion.

Hemodynamic monitoring with two LD probes was performed during transient MCA occlusion, as shown in Fig. 1. The position of the probes was decided according to the rat cerebral vascular territories and verified by gelatin-ink perfusion experiments (Fig. 1A). Probe 1 (bregma -1 mm, 5

mm from midline) was positioned within the central MCA territory, while Probe 2 (bregma +2 mm, 2 mm from midline) was positioned in the borderzone territory between the cortical branches of ACA and MCA to monitor anterior circulation leptomeningeal collaterals. Multi-site cerebral perfusion monitoring was performed during the entire period that the animals remained under anesthesia (Fig. 1C and 1D).

Mean perfusion deficit after MCA occlusion in Probe 2 was significantly lower ($p<0.0001$) and more variable compared to Probe 1 (Fig. 1B). Mean reperfusion values did not differed significantly between the two probes (approximately 92% of baseline, see Fig. 1B) and were not correlated to outcome (data not shown).

Arterial pressure was continuously monitored (Fig. 1E) and did not show significant changes during MCA occlusion (mean arterial pressure 114 mmHg; intra-subject SD 6 mmHg; inter-subject SD 19 mmHg; see Supplementary Fig. 1).

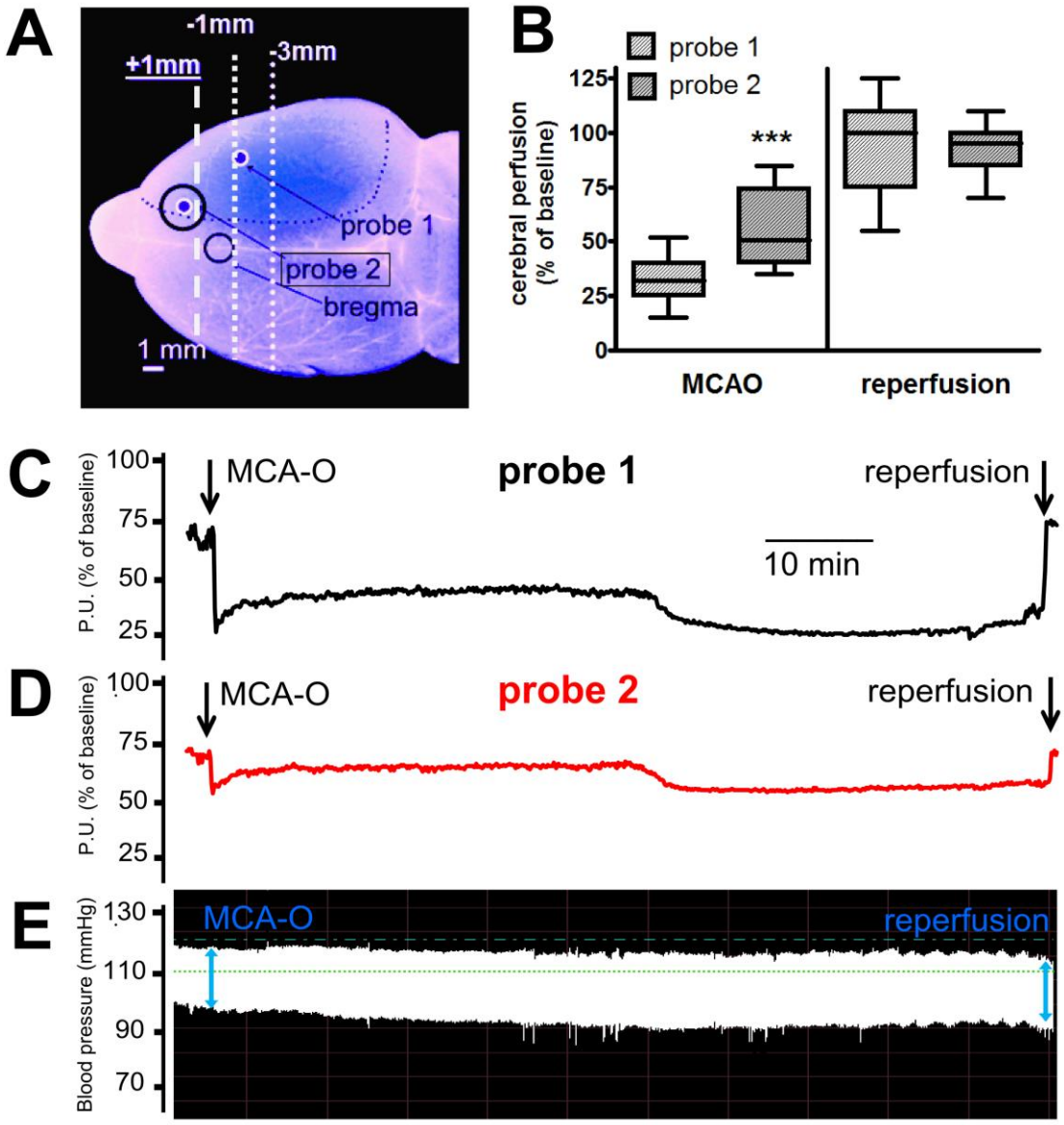

Figure 1.

Hemodynamic monitoring of intracranial collateral flow (anterior circulation leptomeningeal collaterals). **A.** Representative brain perfused with gelatin-ink solution after 90 minutes ischemia, without reperfusion (intraluminal filament was left in place). After colour-inversion, ischemic (not-perfused) area appeared intensely blue-coloured, while the rest of the brain appeared violet with white-stained vessels. The positions of the two laser doppler probes are shown, with reference to their underlying MCA territory (blue dotted line) and bregma. Probe 1 = central MCA territory (-1 mm from bregma, 5 mm from midline); Probe 2 = medial MCA-ACA borderzone territory (+2 mm from bregma, 2 mm from midline). Levels of sections for HSP70 immunostaining (bregma +1, -1 and -3) are shown (white dotted lines). **B.** Perfusion deficit (% of baseline) in the central MCA territory (probe 1) and in the MCA-ACA borderzone territory (probe 2) during MCA-O and reperfusion (n=25). Laser-doppler tracings are shown from a representative animal showing a larger perfusion deficit in Probe 1 (**C**) compared to Probe 2 (**D**) during MCAO, suggesting functionally active intracranial collaterals under ischemic conditions. **E.** Representative tracing of invasive blood pressure monitoring during MCA-O and reperfusion. *** $p < 0.0001$ compared to probe 1. MCA = middle cerebral artery. MCA-O= middle cerebral artery occlusion. ACA = anterior cerebral artery. P.U. = perfusion units.

A biosignal fluctuation analysis of cerebral perfusion tracings, before and after MCA occlusion, showed that the degree of auto-correlation was similar in both probes in the pre-ischemic period, while differed significantly during ischemia (Fig. 2). Although the auto-correlation coefficient increased in both probes compared to the pre-ischemic period, a significantly larger increase was observed in Probe 1 (approximately tripled; $p<0.001$ versus pre-ischemic values) compared to Probe 2 (approximately doubled; $p<0.05$ versus pre-ischemic values) during ischemia.

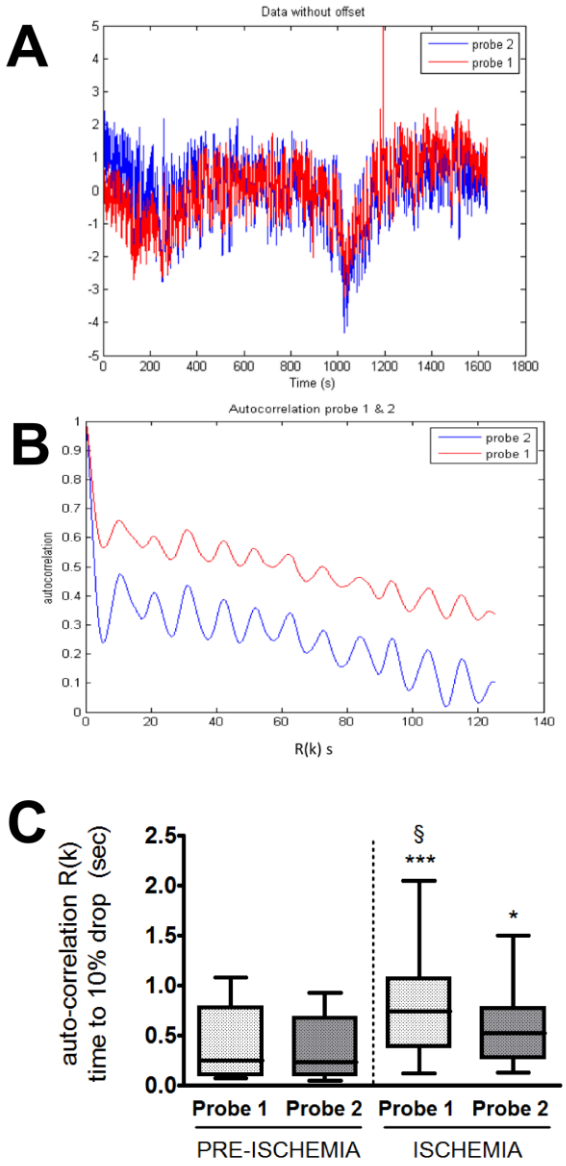

Figure 2.

Biosignal fluctuation analysis of cerebral perfusion in the central MCA territory (probe 1) and in the MCA-ACA borderzone territory (probe 2) at baseline and during MCAO. Regions of interests (ROIs) of Laser Doppler tracings were selected and averaged for offset (**A**). Self-memory of the signal was calculated as expressed as auto-correlation analysis over time for probe 1 and probe 2 (**B**). Self-

memory of the signal was quantified (**C**) as the time to 10% drop in auto-correlation for probe 1 and probe 2, either before ischemia and during MCA-O. *** $p < 0.001$ compared to pre-ischemic Probe 1. * $p < 0.05$ compared to pre-ischemic Probe 2. § $p < 0.05$ compared to ischemic Probe 2. MCA = middle cerebral artery. MCAO= middle cerebral artery occlusion. ACA = anterior cerebral artery. r(K) = auto-correlation function.

Topography of the molecular penumbra.

HSP70 immunoreactivity was assessed 24 hours after reperfusion at sections bregma +1, -1 and -3. Immunofluorescent triple staining confirmed that neuronal HSP70 labeling and apoptotic neuronal nuclei were mutually exclusive, confirming that HSP70 positive cells represented surviving neurons (Fig. 3; see Supplementary Fig. 2 for details on the transition zone between ischemic core and penumbra).

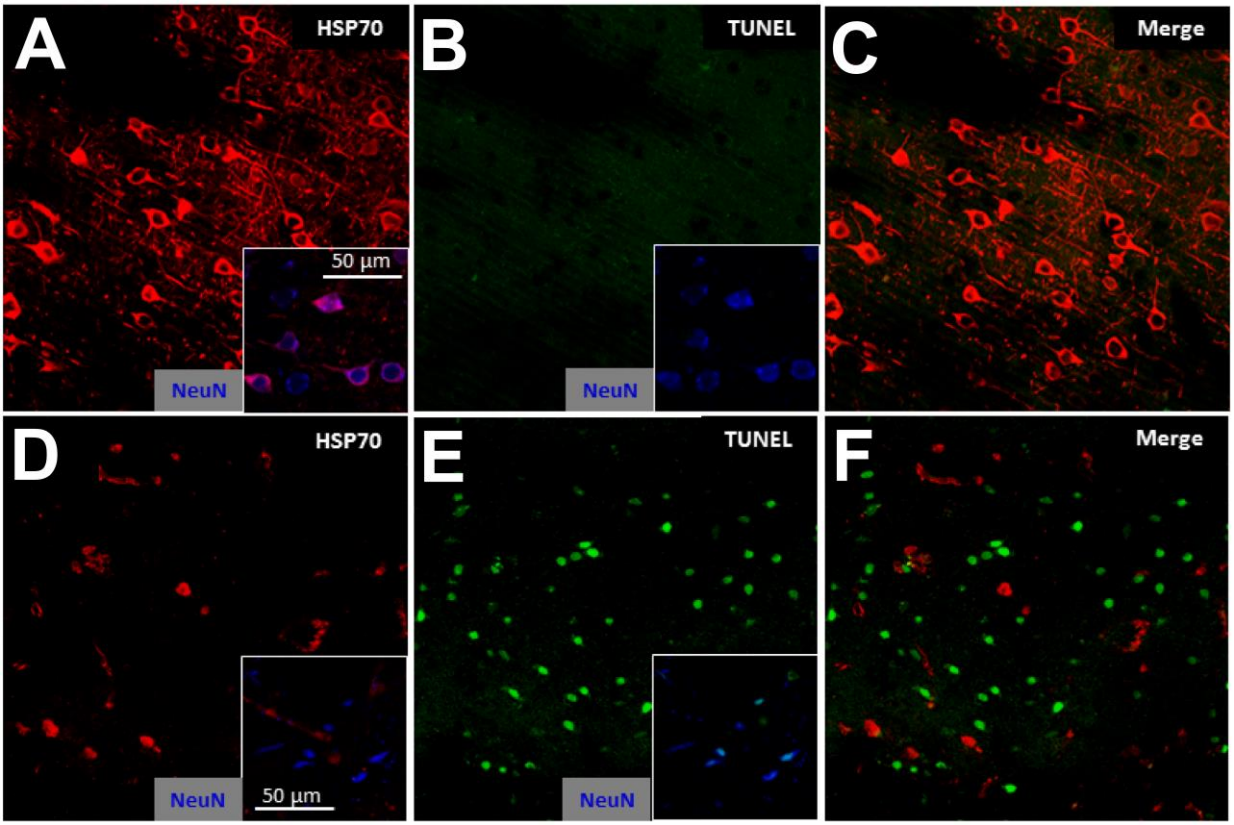

Figure 3.

Triple staining immunohistochemical characterization of the post-reperfusion (24 hours) penumbra. Penumbral areas showed HSP70-immunoreactive cells, co-labeling with the neuronal cell marker Neu-N, and absence of TUNEL-positive nuclei (**A-C**). Ischemic core areas showed TUNEL-positive nuclei, co-labeled with Neu-N, and absence of HSP70-immunoreactive cells with neuronal co-labeling (**D-F**). Sparse HSP70-positive non-neuronal cells were observed in the ischemic core, which did not co-localize with TUNEL-positive nuclei. Representative micrographic pictures are shown.

The pattern of HSP70 staining was consistently different in the cortex compared to striatum (Fig. 4A). In particular, cortical staining showed discrete areas of intensely marked cell clusters (Fig. 4B and 4C), whereas sparse single stained cells were observed in the striatum (Fig. 4D and 4E). Mapping of cortical cell clusters allowed visualizing the topographical distribution of the penumbra in the cortex, which consisted in multiple areas with considerable fragmentation and variable degree of overlaps among different animals (Fig. 4F).

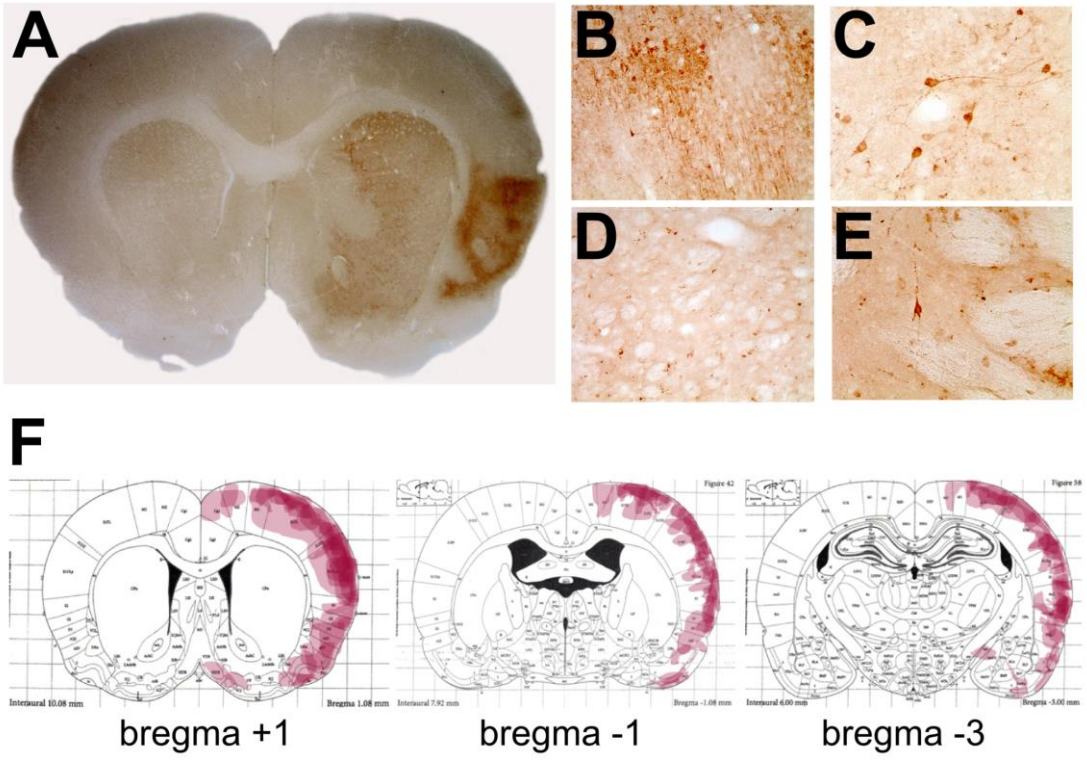

Figure 4.

Morphology and topographic distribution of post-reperfusion penumbra. **A**. Representative picture of HSP70 staining 24 hours after transient MCA-O (90 minutes) on brain section at bregma +1. Higher magnification pictures showing HSP70-positive cells with neuronal morphology, which were observed in clusters in the cortex (**B** 10X; **C** 20X) and as single cells in the striatum (**D** 10X; **E** 20X). **F.** Topographical mapping of HSP70-immunoreactive cell clusters in the cortex at bregma level +1, -1 and -3. Each cell cluster is represented by a single pink-coloured area of variable size. A darker pink colour is the result of variable overlapping degree with adjacent areas from different animals.

Quantification of the molecular penumbra in relation of infarct size and functional deficit.

HSP70 signal was quantified in selected ROIs in the cortex and striatum as shown in Fig. 5A. A positive correlation was observed between HSP70 signal (at section Bregma +1) and infarct volume in both cortex (Fig. 5B; $p < 0.001$; Pearson's *r* 0.67) and striatum (Fig. 5D; $p < 0.05$; Pearson's *r* 0.47). This correlation was also observed at other brain sections, namely at Bregma -1 and -3 (Supplementary Figure 3). A negative correlation was observed between HSP70 signal (at section Bregma +1) and neuroscore in both cortex (Fig. 5C; $p < 0.05$; Pearson's *r* -0.49) and striatum (Fig. 5E; $p < 0.01$; Pearson's *r* -0.54).

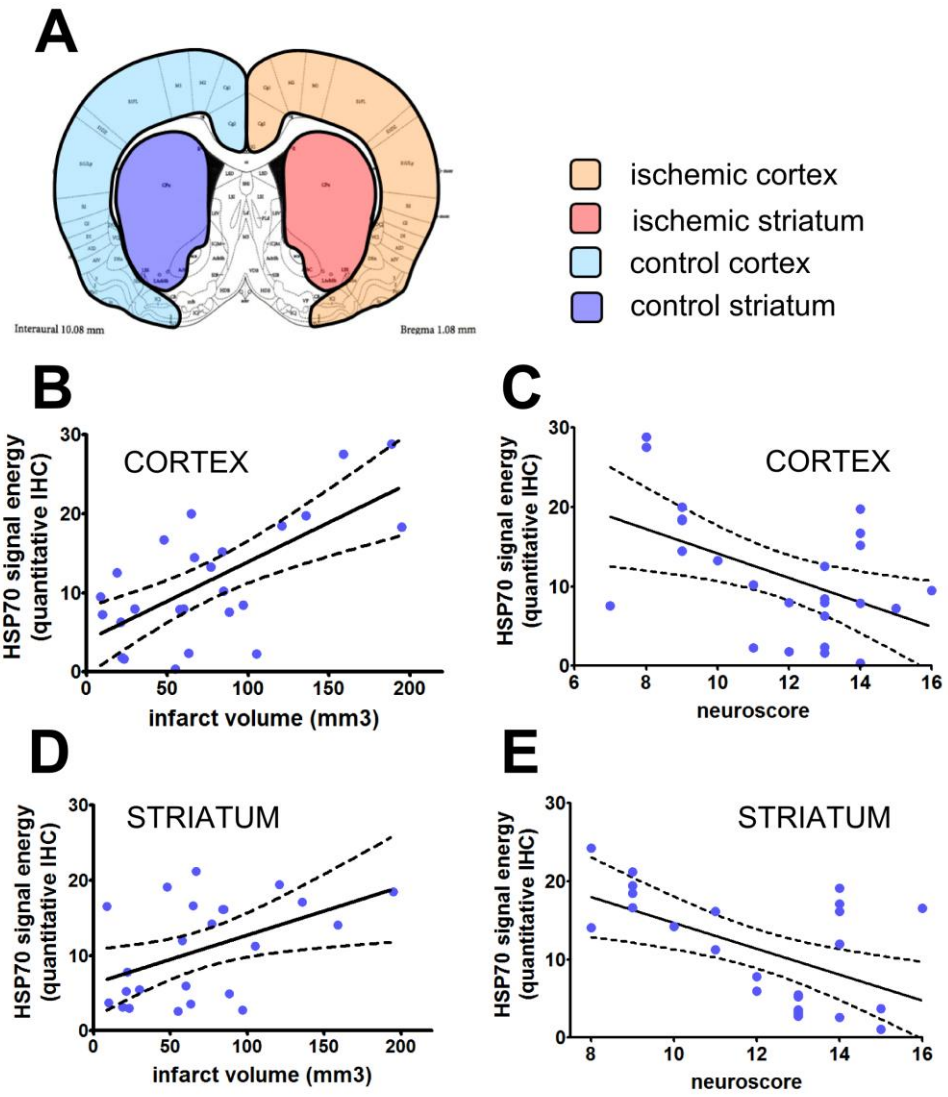

Figure 5.

Quantitative immunohistochemistry of HSP70 after transient MCA-O in relation to structural and functional outcome. **A.** Representation of the four selected region of interests (ROIs) in section bregma +1, which were selected for quantification of HSP70

immunoreactivity using a dedicated software for calculating the mathematical energy of HSP70 signal. **B**. A positive correlation ($p < 0.001$, Pearson's r 0.67) was observed between HSP70 energy signal in the cortex (section bregma +1) and corresponding infarct volume. **C**. A negative correlation ($p < 0.05$, Pearson's r -0.49) was observed between HSP70 energy signal in the cortex (section bregma +1) and corresponding neuroscore. **D**. A positive correlation ($p < 0.05$, Pearson's r 0.47) was observed between HSP70 energy signal in the striatum (section bregma +1) and corresponding infarct volume. **E**. A negative correlation ($p < 0.01$, Pearson's r -0.54) was observed between HSP70 energy signal in the striatum (section bregma +1) and corresponding neuroscore. IHC = immunohistochemistry.

Quantification of the molecular penumbra in relation of intracranial collateral flow.

No correlation was observed between HSP70 signal (at section Bregma +1) and cerebral perfusion in Probe 1 in both cortex (Fig. 6A) and striatum (Fig. 6B). Conversely, a negative correlation was observed between HSP70 signal (at section Bregma +1) and cerebral perfusion in Probe 2 in both cortex (Fig. 6C; $p < 0.01$; Pearson's r -0.54) and striatum (Fig. 6D; $p < 0.05$; Pearson's r -0.42). Interestingly, this correlation was gradually lost in more distant brain sections, namely Bregma -1 and -3 (Supplementary Fig. 4). A negative correlation ($p < 0.001$; Pearson's r -0.62) was observed between infarct volume and cerebral perfusion in Probe 2, while this was not observed for Probe 1 (Supplementary Fig. 5).

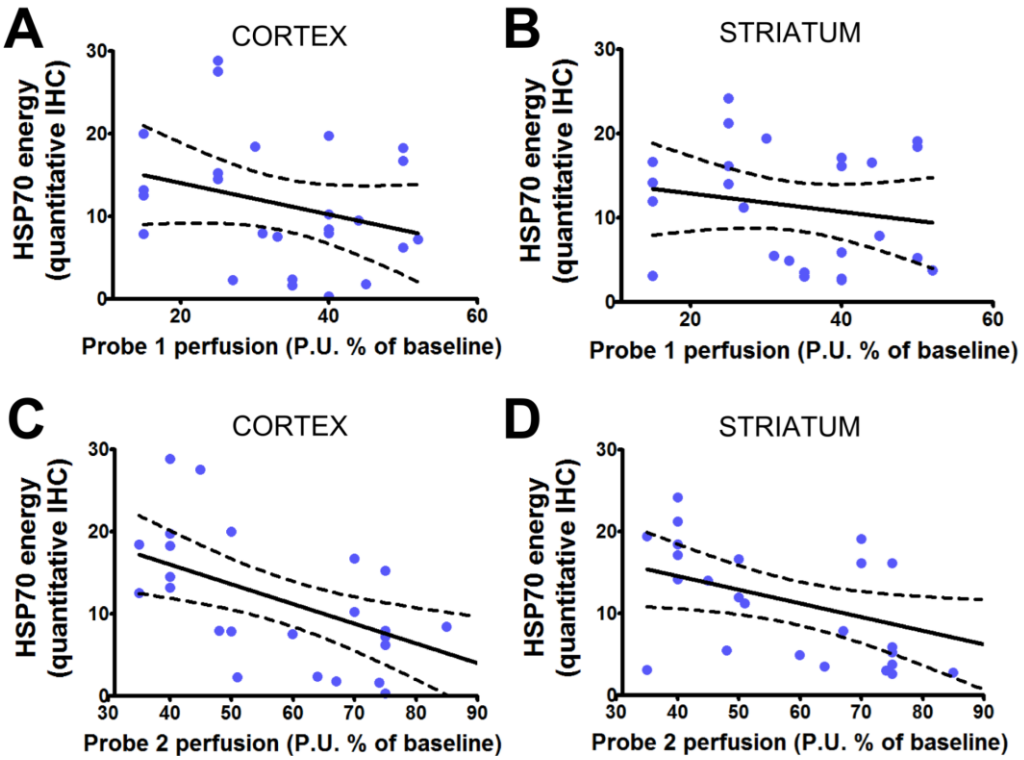

Figure 6.

Correlation between HSP70 energy signal and hemodynamic monitoring in probe 1 (central MCA territory) and probe 2 (MCA-ACA borderzone territory). **A.** No correlation was observed between perfusion values in probe 1 during MCA occlusion and HSP70 energy signal in the cortex (bregma section +1). **B.** No correlation was observed between perfusion values in probe 1 during MCA occlusion and HSP70 energy signal in the striatum (bregma section +1). **C.** A negative correlation ($p < 0.01$, Pearson's r -0.54) was observed between perfusion values in probe 2 during MCA occlusion and HSP70 energy signal in the cortex (bregma section +1). **D.** A negative correlation ($p < 0.05$, Pearson's r -0.42) was observed between perfusion values in probe 2 during MCA occlusion and HSP70 energy signal in the striatum (bregma section +1). IHC= immunohistochemistry. P.U.= perfusion units. MCA= middle cerebral artery. ACA= anterior cerebral artery.

Discussion

The functional performance of intracranial collaterals is crucially involved in the pathophysiology of acute ischemic stroke (Liebeskind et al., 2012). Functionally active cerebral collaterals have been associated with reduced penumbra loss (Jung et al., 2013) and better outcomes (Cortijo et al., 2014) in acute stroke patients, even with delayed reperfusion.

Therapeutic modulation of cerebral collateral flow is being proposed (Shuaib et al., 2011) and may be used for widening the therapeutic window for recanalization and enhancing delivery of neuroprotective drugs.

The endurance of "tissue at risk" in the setting of hypoperfusion has been postulated to be dependent on collateral flow in humans (Liebeskind et al., 2013). Nonetheless, the relationship between the degree of collateral perfusion and the extent and evolution of ischemic penumbra in acute ischemic stroke has not been investigated in experimental studies and remains an important unsolved issue.

The definition of penumbral tissue in current stroke research mostly relies on MRI imaging in humans (Schlaug et al., 1999) and animal models (Reid et al., 2012), applying diffusion-weighted (DWI) and perfusion-weighted imaging (PWI) and calculating the PWI-DWI mismatch. This method has been demonstrated to predict clinical outcome and final infarct size in stroke patients undergoing endovascular therapy (Lansberg et al., 2012; Wheeler et al., 2013). Nonetheless it is recognized that PWI-DWI mismatch cannot define the penumbra with absolute accuracy in humans (Heiss, 2011) and in animals (Duong, 2012) and remains unsatisfactory for pathophysiological studies assessing tissue viability and response to injury.

Moreover, the pattern of DWI lesions and PWI-DWI mismatch in the first hours after acute ischemic stroke has been shown to display significant inter-individual variability and evolve over time (Olivot et al., 2009).

Our experimental study investigated the dynamic relationship between cerebral collateral flow and the development of molecular penumbra, after intraluminal proximal MCA occlusion (90 minutes) followed by 24 hours reperfusion.

We mapped and quantified the ischemic penumbra by molecular activation of HSP70. The extent of this "molecular penumbra" was related to the vascular perfusion deficit in the acute phase and to the structural and functional outcome at 24 hours.

Our findings indicate that good collateral flow during MCA occlusion reduces the molecular activation associated with penumbral tissue, providing complete protection from ischemic injury in variable areas of the cortex and striatum, if reperfusion is achieved. Conversely, poor collateral status is associated with a greater extent of both ischemic core and molecular penumbra.

This new scenario of the interplay between cerebral collateral flow and ischemic penumbra might have potential translational applications. Therapeutic strategies aimed to enhance collateral circulation early after arterial occlusion may completely prevent the "ischemic cascade" in a significant amount of brain tissue, expanding the therapeutic effect of recanalization therapies and reducing their risks.

The study of intracranial collaterals and cerebral hemodynamic changes in experimental ischemic stroke remains largely unexplored (Sutherland et al., 2011), mostly because of the technical difficulties to obtain a quantitative assessment of the dynamic response of collateral vessels. Our group recently developed an optimized system for cerebral perfusion monitoring in rats (Beretta et al., 2013), demonstrating that leptomeningeal collateral flow showed significant variability during MCAO in rats and is a strong predictor of "hard outcomes" such as infarct size and functional deficit (Riva et al., 2012), while its relationship to the penumbra remained to be explored.

Our findings confirm the utility of multi-site LD monitoring in the central and peripheral MCA territory as an easy and reliable method to quantify cerebral collateral flow during proximal MCA occlusion. A gradient of severity between the two probes was observed either by relative perfusion deficit or biosignal fluctuation analysis. In particular, hemodynamic monitoring in LD Probe 2, in the territory of MCA-ACA leptomeningeal branches, showed a cortical area with a lower perfusion deficit, higher inter-individual variability and larger fluctuations of the biosignal, compared to LD Probe 1 in the central MCA territory.

In most animals the topographical mapping of molecular penumbra (HSP70 positive areas after 24 hours of reperfusion) revealed multiple patchy areas with irregular distribution, not limited to the peri-lesional zone; this is in contrast with the final infarct, which invariably consisted in a single

lesion of variable size. Our results confirmed that HSP70-stained neurons are a separate population from neurons undergoing selective cell death (TUNEL-stained neurons), in agreement with previous reports (Del Zoppo et al., 2011).

Surprisingly, we observed a striking correlation between the extent of molecular penumbra and stroke severity, in term of both infarct volume and neuroscore. Notably, small infarcts (mostly limited to the striatum) were associated with little (if any) penumbral tissue, whereas larger infarcts involving the striatum and cortex were associated with larger areas of molecular penumbra. No animals exhibited a pattern of small ischemic core surrounded by large penumbral areas.

A strong correlation was observed between the extent of molecular penumbra and the severity of perfusion deficit in the peripheral MCA territory (Probe 2), which reflects intracranial collateral perfusion. Interestingly, no correlation was observed the extent of molecular penumbra and perfusion deficit in the central MCA territory (Probe 1). In other terms, the presence of good collaterals reduced the extent of both molecular penumbra and ischemic core at 24 hours, increasing the amount of uninjured (completely "saved") cerebral tissue.

Two additional results strengthen the specificity of these findings: first, the correlation between perfusion deficit in Probe 2 and HSP70-stained areas is stronger at level Bregma +1 (the nearest of the Probe 2 position) and gradually diminishes with the distance, i.e. Bregma -1 and -3; second, arterial blood pressure neither show significant changes during the ischemic phase (90 minutes) nor correlated with the final stroke outcome in our series.

The major limitation of our study is that acute penumbral MRI imaging using DWI-PWI mismatch has not been performed and molecular penumbra was assessed 24 hours after reperfusion, as this was necessary to obtain a useful HSP70 staining. However, cerebral collateral flow was the main focus of the study and this can be quantified more reliably with multi-site LD monitoring than with current MRI technology in small animals. The relationship between acute penumbral MRI imaging and molecular penumbra assessed by HSP70 staining is beyond the scope of this study and is currently being explored in new experiments. Although acute MRI-defined penumbra could be

expected to be larger than molecular penumbra after 24 hours of reperfusion (due to the progressive recruitment of penumbra into infarct core), this is unlikely to change the major findings of the present study.

Conclusions

The degree of cerebral collateral perfusion inversely correlated with both ischemic core and molecular penumbra during transient proximal MCA occlusion. Our findings prompt the development of collateral therapeutics to provide tissue-saving strategies in the hyper-acute phase of ischemic stroke prior to recanalization therapy.

Acknowledgements

We thank Dr. Virginia Rodriguez Menendez for technical assistance with immunohistochemistry and Miss Elena Pirovano for figure preparation. This study was supported by the Italian Ministry of University and Research (MIUR) and Université Lyon 1. These funding sources were not involved in the study design, collection, analysis and interpretation of data, writing of the report or decision to submit the present article for publication.

Conflict of interest

The authors declare no conflict of interest.

Supplementary Figure Captions

Supplementary Figure 1. Representative view of the "transition zone" between intact and ischemic tissue 24 hours after of transient middle cerebral artery occlusion. Brain sections were stained with triple immunofluorescence for NeuN (neuronal cells; blue), HSP70 (penumbra; red) and TUNEL (apoptotic nuclei; green). Healthy neurons (NeuN+, HSP70-, TUNEL-), penumbral neurons (NeuN+, HSP70+, TUNEL-; open arrows) and apoptotic neurons (NeuN+, HSP70-, TUNEL+; small arrows) appear as separate cell populations with a clear topographical demarcation.

Supplementary Figure 2. Invasive blood pressure monitoring during transient middle cerebral artery occlusion (MCAO). Upper graph shows mean blood pressure values (n=12) every 10 minute intervals, demonstrating no significant variation of blood pressure over the ischemic period of 90 minutes. Lower graph shows mean blood pressure values of each animal, demonstrating small intra-subject variability of blood pressure during the entire ischemic period.

Supplementary Figure 3. Quantitative immunohistochemistry of HSP70 after transient MCAO in relation to infarct volume in sections bregma -1 and -3. **B**. A positive correlation was observed between HSP70 energy signal in the cortex and corresponding infarct volume for brain sections at bregma -1 (left graph; $p < 0.01$, $r = 0.52$) and bregma -3 (right graph; $p < 0.05$, $r = 0.48$). IHC = immunohistochemistry.

Supplementary Figure 4. Quantitative immunohistochemistry of HSP70 after transient MCAO in relation to cerebral collateral flow (probe 2). No correlation was observed between HSP70 energy signal in the cortex at bregma -1 (left graph) and bregma -3 (right graph) and cerebral collateral flow (measured at bregma +1). IHC = immunohistochemistry.

Supplementary Figure 5. Correlation between infarct volume and cerebral perfusion in probe 1 (central MCA territory) and probe 2 (MCA-ACA borderzone territory) during MCA occlusion. No correlation was observed between infarct volume and cerebral perfusion in probe 1. A negative correlation ($p = 0.001$; $r = -0.62$) was observed between infarct volume and cerebral perfusion in probe 2. MCA = middle cerebral artery. ACA = anterior cerebral artery.

References

Armitage GA, Todd KG, Shuaib A, Winship IR. Laser speckle contrast imaging of collateral blood flow during acute ischemic stroke. J Cereb Blood Flow Metab 2010; 30: 1432-6.

Bang OY, Saver JL, Buck BH, Alger JR, Starkman S, Ovbiagele B, et al. Impact of collateral flow on tissue fate in acute ischaemic stroke. J Neurol Neurosurg Psychiatry 2008; 79(6): 625-9.

Bang OY, Saver JL, Kim SJ, Kim GM, Chung CS, Ovbiagele B, et al. Collateral flow predicts response to endovascular therapy for acute ischemic stroke. Stroke 2011; 42(3): 693-9.

Baron JC. Mapping the ischaemic penumbra with PET: implications for acute stroke treatment. [Review]. Cerebrovasc Dis 1999; 9: 193–201.

Beretta S, Riva M, Carone D, Cuccione E, Padovano G, Rodriguez Menendez V, et al. Optimized system for cerebral perfusion monitoring in the rat stroke model of intraluminal middle cerebral artery occlusion. J Vis Exp 2013; (72). pii: 50214. doi: 10.3791/50214.

Branston NM, Symon L, Crockard HA, Pasztor E. Relationship between the cortical evoked potential and local cortical blood flow following acute middle cerebral artery occlusion in the baboon. Exp Neurol 1974; 45: 195–208.

Brunner F, Tomandl B, Hanken K, Hildebrandt H, Kastrup A. Impact of collateral circulation on early outcome and risk of hemorrhagic complications after systemic thrombolysis. Int J Stroke 2012 Oct 23. doi: 10.1111/j.1747-4949.2012.00922.x.

Cortijo E, Calleja AI, García-Bermejo P, Mulero P, Pérez-Fernández S, Reyes J, et al. Relative Cerebral Blood Volume as a Marker of Durable Tissue-at-Risk Viability in Hyperacute Ischemic Stroke. Stroke 2014; 45(1): 113-8.

del Zoppo GJ, Sharp FR, Heiss WD, Albers GW. Heterogeneity in the penumbra. [Review]. J Cereb Blood Flow Metab 2011; 31: 1836-51.

Duong TQ. Multimodal MRI of experimental stroke. Transl Stroke Res 2012; 3: 8-15.

Garcia JH, Wagner S, Liu KF, Hu XJ. Neurological deficit and extent of neuronal necrosis attributable to middle cerebral artery occlusion in rats. Statistical validation. Stroke 1995; 26: 627-34

Heiss WD. The ischemic penumbra: correlates in imaging and implications for treatment of ischemic stroke. The Johann Jacob Wepfer award 2011. Cerebrovasc Dis 2011; 32: 307–20.

Hossmann KA. Viability thresholds and the penumbra of focal ischemia. Ann Neurol 1994; 36: 557–65.

Humeau-Heurtier A, Guerreschi E, Abraham P, Mahé G. Relevance of laser Doppler and laser speckle techniques for assessing vascular function: state of the art and future trends. IEEE Trans Biomed Eng 2013; 60: 659-66.

Humeau A, Fizanne L, Roux J, Asfar P, Cales P, Rousseau D et al. Linear, nonlinear analyses of laser Doppler flowmetry signals recorded during isoflurane-induced anaesthesia in healthy rats. J Vasc Res 2008 (Suppl 2); 45: 82.

Jung S, Gilgen M, Slotboom J, El-Koussy M, Zubler C, Kiefer C, et al. Factors that determine penumbral tissue loss in acute ischaemic stroke. Brain 2013; 136: 3554-60.

Lansberg MG, Straka M, Kemp S, Mlynash M, Wechsler LR, Jovin TG, et al. MRI profile and response to endovascular reperfusion after stroke (DEFUSE 2): a prospective cohort study. Lancet Neurol 2012; 11: 860-7.

Liebeskind DS. Collateral circulation. [Review]. Stroke 2003; 34: 2279-84.

Liebeskind DS. Collateral perfusion: time for novel paradigms in cerebral ischemia. Int J Stroke 2012; 7: 309-10.

Liebeskind DS. Trials of endovascular therapies or collaterals? Int J Stroke 2013; 8: 258-9.

Liu W, Xu G, Yue X, Wang X, Ma M, Zhang R, et al. Hyperintense vessels on FLAIR: a useful non-invasive method for assessing intracerebral collaterals. Eur J Radiol 2011; 80: 786-91.

Maas MB, Lev MH, Ay H, Singhal AB, Greer DM, Smith WS. Collateral vessels on CT angiography predict outcome in acute ischemic stroke. Stroke 2009; 40: 3001-5.

Manning NW, Campbell BC, Oxley TJ, Chapot R. Acute Ischemic Stroke: Time, Penumbra, and Reperfusion. Stroke 2014; 45: 640-4.

Matkowskyj KA, Schonfeld D, Benya RV. Quantitative immunohistochemistry by measuring cumulative signal strength using commercially available software photoshop and matlab. J Histochem Cytochem 2000; 48: 303-12.

Menon BK, Smith EE, Modi J, Patel SK, Bhatia R, Watson TW, et al. Regional leptomeningeal score on CT angiography predicts clinical and imaging outcomes in patients with acute anterior circulation occlusions. Am J Neuroradiol 2011; 32: 1640-5.

Miteff F, Levi CR, Bateman GA, Spratt N, McElduff P, Parsons MW. The independent predictive utility of computed tomography angiographic collateral status in acute ischaemic stroke. Brain 2009; 132: 2231-8.

Olivot JM, Mlynash M, Thijs VN, Purushotham A, Kemp S, Lansberg MG, et al. Geography, structure, and evolution of diffusion and perfusion lesions in Diffusion and perfusion imaging Evaluation For Understanding Stroke Evolution (DEFUSE). Stroke 2009; 40: 3245-51.

Paxinos G, Watson C, editors. The Rat Brain in Stereotaxic Coordinates, 6th edition. San Diego: Academic Press; 2007.

Qureshi AI, El-Gengaihi A, Hussein HM, Suri MF, Liebeskind DS. Occurence and variability in acute formation of leptomeningeal collaterals in proximal middle cerebral artery occlusion. J Vasc Interv Neurol 2008; 1: 70-2.

Reid E, Graham D, Lopez-Gonzalez MR, Holmes WM, Macrae IM, McCabe C. Penumbra detection using PWI/DWI mismatch MRI in a rat stroke model with and without comorbidity: comparison of methods. J Cereb Blood Flow Metab 2012; 32: 1765-77.

Riva M, Pappadà GB, Papadakis M, Cuccione E, Carone D, Menendez VR, et al. Hemodynamic monitoring of intracranial collateral flow predicts tissue and functional outcome in experimental ischemic stroke. Exp Neurol 2012; 233: 815-20.

Schlaug G, Benfield A, Baird AE, Siewert B, Lovblad KO, Parker RA, et al. The ischemic penumbra: operationally defined by diffusion and perfusion MRI. Neurology 1999; 53: 1528-37.

Sharp FR, Lu A, Tang Y, Millhorn DE. Multiple molecular penumbras after focal cerebral ischemia. [Review]. J Cereb Blood Flow Metab 2000; 20: 1011-32.

Shuaib A, Butcher K, Mohammad AA, Saqqur M, Liebeskind DS. Collateral blood vessels in acute ischaemic stroke: a potential therapeutic target. [Review]. Lancet Neurol 2011; 10: 909-21.

Sutherland BA, Papadakis M, Chen RL, Buchan AM. Cerebral blood flow alteration in neuroprotection following cerebral ischemia. J Physiol 2011; 589: 4105-14.

Wheeler HM, Mlynash M, Inoue M, Tipirneni A, Liggins J, Zaharchuk G, et al. Early diffusion-weighted imaging and perfusion-weighted imaging lesion volumes forecast final infarct size in DEFUSE 2. Stroke 2013; 44: 681-5.